Correspondence

Analysis of a Two-Section Coupler*

The use of single-section quarter wavelength TEM mode directional couplers having excellent wide-band performance is well known.[1] A method for decreasing the coupling variation with frequency by cascading three quarter wavelength couplers has also been described.[2] The purpose of this note is to analyze, for loose coupling, the behavior of a two quarter wave section coupler and compare the results with a coupler consisting of three sections.

The basic coupler configuration is shown in Fig. 1. For an incident voltage of unity, the coupled voltage V_c can be written as (neglecting the time dependence)

$$V_c = j\beta \int k(x) e^{-j2\beta x}, \qquad (1)$$

where $|k(x)|^2 \ll 1$

$$V_c = j\beta\left[\int_0^{L_1} k_1 e^{-j2\beta x}dx + \int_0^{L_2} k_2 e^{-j2\beta x}dx\right]. \quad (2)$$

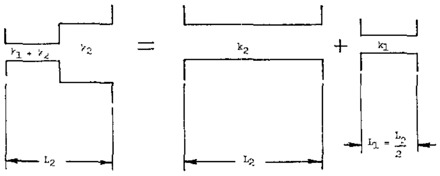

Fig. 1—Superposition of two single-section couplers to form a two-section coupler.

Upon integrating and using the fact that $L_2 = 2L_1$, we obtain

$$V_c = je^{-j\beta L_1}[k_1 \sin \beta L_1 + e^{-j\beta L_1} k_2 \sin 2\beta L_1]. \quad (3)$$

By letting $k_2 = 0$, the familiar result for the single-section quarter wave coupler is obtained.

One can note from (3) that the phase shift of the coupled wave is no longer 90°, as it would be for the single-section or three-section couplers.

The quantity of interest is $|V_c|^2$. Expanding the portion of (3) in the brackets and squaring the real and imaginary parts, we have

$$|V_c|^2 = k_1^2 \sin^2\theta + 2k_1k_2 \sin\theta \cos\theta \sin 2\theta + k_2^2 \cos^2\theta \sin^2 2\theta + k_2^2 \sin^2\theta \sin^2 2\theta, \quad (4)$$

where $\theta = \beta L_1$.

Combining terms

$$|V_c|^2 = \sin^2\theta[k_1^2 + 4k_1k_2\cos^2\theta + 4k_2^2\cos^2\theta] \quad (5)$$

or

$$|V_c|^2 = k_1^2 \sin^2\theta[1 + 4r(1+r)\cos^2\theta], \quad (6)$$

where $r = k_2/k_1$.

In Fig. 2, the bandwidth ratio of the two-section coupler is plotted as a function of the coupling variation for an equal ripple response. A comparison with the three-section coupler shows that, for practical purposes, one does not buy much in the way of improved performance over a two-section coupler by going to the extra section. For example, the coupling variations for a three-to-one bandwidth are 0.21 and 0.26 db respectively, or a difference of only 0.05 db. However, both three- and two-section couplers exhibit substantially better performance than a single-section coupler. Fig. 3 gives the coupling variation as a function of r.

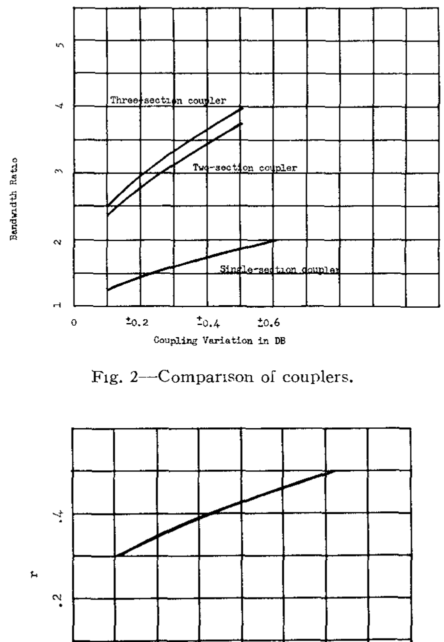

Fig. 2—Comparison of couplers.

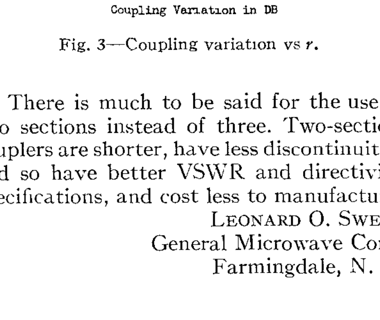

Fig. 3—Coupling variation vs r.

There is much to be said for the use of two sections instead of three. Two-section couplers are shorter, have less discontinuities and so have better VSWR and directivity specifications, and cost less to manufacture.

Leonard O. Sweet
General Microwave Corp.
Farmingdale, N. Y.

* Received February 14, 1962.

[1] B. M. Oliver, "Directional electromagnetic coupling," Proc. IRE, vol. 42, pp. 1686–1692; November, 1954.

[2] J. K. Shimizu and E. M. T. Jones, "Coupled-transmission-line directional couplers," IRE Trans. on Microwave Theory and Techniques, vol. MTT-6, pp. 403–410; October, 1958.

Measuring the ω-β Diagram of Periodic Structures*

One of the most important properties of a periodic structure is the shape of the ω-β diagram. A common technique for measuring the ω-β diagram is to form a resonant section by placing shorting planes at positions of symmetry within the periodic structure and to observe the resonant frequencies of the resulting resonator.[1] Discussed in this correspondence is a technique wherein the far end of the periodic structure is shorted and the positions of nulls of voltage on an input line are observed as frequency is varied. From these nulls it is possible to determine the frequencies where the electrical length of the loaded structure is a multiple of π radians. Basically, it is a procedure for graphically determining points on the ω-β diagram.

As an example of the technique, consider a periodic structure formed by a TEM line with six loading elements to give five sections as shown in Fig. 1. The unloaded

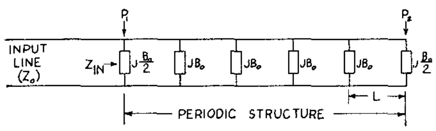

Fig. 1—Uniform periodic structure with five sections.

characteristic impedance of the line used in the periodic structure is assumed to be the same as that of the input line. Following the work of Slater,[2] the equation for the phase constant β_0 per section of the periodic structure is

$$\cos \beta_0 L = \cos \beta L - \frac{B_0 Z_0}{2} \sin \beta L \quad (1)$$

where β is the phase constant per length L of the unloaded line and Z_0 is the unloaded characteristic impedance. Assuming capacitive loading, for example, $B_0 = \omega C_0$ and (1) becomes

$$\cos \beta_0 L = \cos \beta L = \beta L(K_1) \sin \beta L, \quad (2)$$

where

$$K_1 = \frac{C_0 Z_0}{2L\sqrt{\mu_0 \epsilon_0}}. \quad (3)$$

Continuing with the example and taking

* Received February 22, 1962. This work was supported in part by the U. S. Army (Ordnance Corps) under Contract DA-01-009-ORD-858.

[1] D. A. Watkins, "Topics in Electromagnetic Theory," John Wiley and Sons, Inc., New York, N. Y., pp. 9–10; 1958.

[2] J. C. Slater, "Microwave Electronics," D. Van Nostrand Co., Inc., New York, N. Y., pp. 177–186; 1950.

$K_1=0.4$, the expected ω-β diagram calculated from (2) is shown in Fig. 2. Since βL is a known function of ω in a given structure, the ordinate of Fig. 2 could have been plotted in terms of ω.

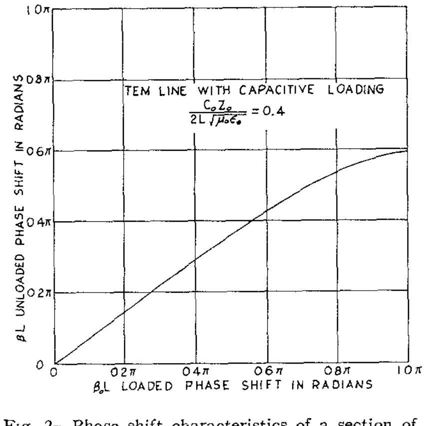

Fig. 2—Phase shift characteristics of a section of a periodic structure with loading elements spaced L distance apart.

Consider now the situation when the far end of the periodic structure is shorted at P_2. The impedance seen by the input line at P_1 is obtained from the results of Slater

$$Z_{in} = jZ_0 \frac{\sin \beta L}{\sin \beta_0 L} \tan 5\beta_0 L, \tag{4}$$

where the term

$$Z_0 \frac{\sin \beta L}{\sin \beta_0 L}$$

is the image impedance of the loaded line. Substituting the values of $\beta_0 L$ given by (2) and Fig. 2 into (4) would give the variation of Z_{in} with changes in βL. The null positions in the input line can also be expressed in terms of these values of Z_{in} as follows. The reflection coefficient "seen" by the input line at P_1 is

$$K_r = \frac{Z_{in} - Z_0}{Z_{in} + Z_0}$$

or from (4)

$$K_r = 1 \angle \overline{\pi + 2\arctan\left(-\frac{\sin \beta L}{\sin \beta_0 L}\tan 5\,\beta_0 L\right)}. \tag{5}$$

A null occurs on the input line at a distance S from the point P_1, where

$$-\frac{2S}{\lambda}(2\pi) + 2\arctan\left(-\frac{\sin\beta L}{\sin\beta_0 L}\tan 5\beta_0 L\right) = 0$$

or

$$\frac{S}{\lambda} = \frac{\arctan\left(-\frac{\sin\beta L}{\sin\beta_0 L}\tan 5\beta_0 L\right)}{2\pi}. \tag{6}$$

If the values of S/λ given by (6) were plotted against βL, choosing the solution whose magnitude was less than $\frac{1}{4}$ each time, the cross-over points where $S/\lambda = 0$ would give the frequencies where $5\beta_0\lambda = n\pi$. These would correspond to $\beta_0 L = 0$, 0.2π, 0.4π, 0.6π, 0.8π, and 1.0π in the example under consideration.

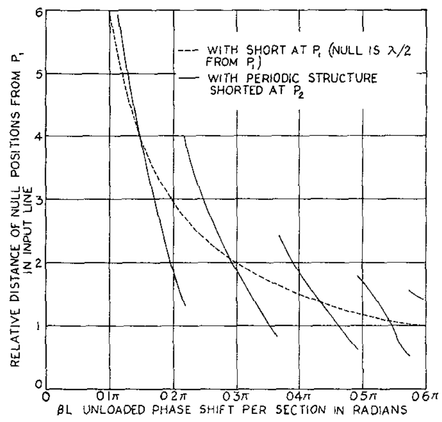

Fig 3—Calculated change of null positions in the input line as the frequency is varied ($\beta L = \omega L\sqrt{\mu_0\epsilon_0}$).

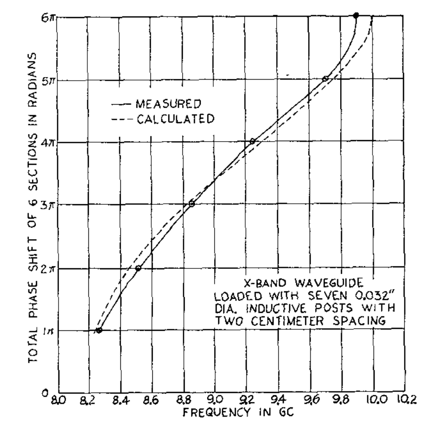

Fig. 4—Comparison of calculated phase shifts of a loaded waveguide with measured values obtained from the null movements.

In an experimental procedure, reference nulls which were a multiple of $\lambda/2$ away from P_1 would be taken and the motion of the nulls of the circuit under test about these would be observed. Fig. 3 shows the expected curves for the example under consideration when the reference null is taken $\lambda/2$ away from point P_1 at each frequency. The intersections of these curves give the values of βL corresponding to $5\beta_0 L = n\pi$ as can be seen by comparing Fig. 3 to Fig. 2. As shown by Fig. 3, the values at the edges of the pass bands are not included by this procedure. In this example, obviously, the reason at the lower edge is the difficulty of including the long wavelengths. At the upper edge, the reason is that the image impedance approaches an infinite value and (4) approaches a finite value instead of zero as might be expected from the tan $5\beta_0 L$ term. However, these edge-points can be located anyway from the knowledge of the pass band.

The application of this technique is not limited to the simple situation shown. For example, the characteristic impedance of the input line need not be the same as that of the loaded line so long as the reference nulls are located correctly. It is not necessary to have the $B_0/2$ matching sections at the end; the same results would be obtained if they were equal to B_0. Other types of loading can be handled as well as waveguide structures. Fig. 4 shows a comparison of experimental and calculated data for a structure consisting of seven 0.032-inch diameter inductive posts in the center of X-band waveguide (1 inch by $\frac{1}{2}$ inch outside dimensions) and spaced 2 cm apart. Although the exact shapes of the curves may vary depending on the actual situation, the technique can be applied to many periodic structures.

The efforts of S. N. James in constructing the circuit and making the measurements and calculations for Fig. 4 are gratefully acknowledged.

ODIS P. MCDUFF
Elec. Engrg. Dept.
University of Alabama
University, Ala

Synthetic Transmission-Line Impedance Transformers*

Somlo[1] has presented a convenient procedure for obtaining the characteristic impedance and length of a single section of lossless transmission line to match two impedances. One impedance and the conjugate of the other are plotted on a circular transmission-line chart, *i.e.*, Smith or Carter chart. A circle is drawn through the two points with its center on the $X=0$ axis. If the circle does not lie entirely within the $R=0$ circle, the two impedances cannot be matched with a single section of lossless transmission line with real characteristic impedance. However, if one does not require that the transmission line have a real characteristic impedance, it can be synthetized by a symmetrical T or π network consisting of either lossless inductances or capacitances.

A graphical procedure for obtaining the parameters of such a section of synthetic transmission line is presented here. The load impedance $\boldsymbol{Z_A}$ and the conjugate of the source impedance $\boldsymbol{Z_B}^*$ are plotted on a circular transmission-line chart, as shown in

* Received April 5, 1962.

[1] P. I. Somlo, "A logarithmic transmission line chart," IRE TRANS. ON MICROWAVE THEORY AND TECHNIQUES (*Correspondence*), vol. MTT-8, p. 463; July, 1960.